Journal of The Electrochemical Society, **153** (2) C127-C132 (2006)
0013-4651/2006/153(2)/C127/6/$15.00 © The Electrochemical Society

Curvature Enhanced Adsorbate Coverage Model for Electrodeposition

T. P. Moffat,* D. Wheeler, S.-K. Kim, and D. Josell[z]

Materials Science and Engineering Laboratory, National Institute of Standards and Technology, Gaithersburg, Maryland 20899, USA

The influence of a catalyst deactivating leveling additive in electrodeposition is explored in the context of the previously developed curvature enhanced accelerator coverage model of superconformal film growth. Competitive adsorption between a rapidly adsorbed suppressor, rate accelerating catalyst, and catalyst-deactivating leveler is examined. Rate equations are formulated where the leveling agent is capable of deactivating the adsorbed catalyst by either direct adsorption from the electrolyte or by deactivation/displacement during surface area reduction that accompanies advancing concave surfaces. The influence of a prototypical cationic surfactant leveler on electrochemical kinetics and feature filling is examined for copper electrodeposition from an electrolyte containing polyethylene glycol-chloride-bis(3-sulfopropyl)disulfide (PEG-Cl-SPS).
© 2006 The Electrochemical Society. [DOI: 10.1149/1.2165580] All rights reserved.

Manuscript submitted May 11, 2005; revised manuscript received September 27, 2005. Available electronically January 11, 2006.

Superconformal copper electrodeposition is widely used in the fabrication of state-of-the-art microelectronic circuitry. Such void-free filling of submicrometer trenches and vias is a consequence of the competitive adsorption dynamics between rate accelerating bis-(3-sulfopropyl) disulfide-chloride (SPS-Cl) and rate suppressing polyethylene glycol-chloride, (PEG-Cl) additives coupled with the effects of local area change. A quantitative description, known as the curvature enhanced accelerator coverage model (CEAC) that provides a direct link between kinetics determined by electroanalytical experiments on planar electrodes and shape-change simulations of feature filling has been developed.[1] In the case of copper electrodeposition, two additives (accelerator-suppressor) are the minimal number required for robust bottom-up feature filling. However, the growth process also results in an overshoot phenomenon, known in industrial circles as momentum plating, which results in excess material buildup above the features of interest. The phenomenon is a strong function of wiring pattern geometry and density with greater buildup occurring over regions that experience the greatest reduction in interfacial area during feature filling, i.e. closely spaced fine trenches.[2,3] The uneven buildup hampers the subsequent chemical mechanical planarization (CMP) subtractive planarization process. As a result a variety of strategies have been developed to control the overshoot process.[4-12] A common theme is the attenuation or removal of accumulated accelerator from the surface immediately after feature filling but prior to bump formation. Manifestations of this strategy range from (*i*) using a dilute deposition rate inhibiting species, often referred to as a leveling agent, that acts to deactivate the accelerating surface species,[4-8] (*ii*) using a two-step process where the bottom-up filling (or a catalyst derivatization) step is followed by deposition in the presence of an inhibiting (and suppressing) species that might or might not act in a similar fashion to that outlined in (*i*)[6,9,10,12] (*iii*) using an oxidation process as implemented in pulse reverse plating to deactivate the accelerating additive,[6,10] and (*iv*) using mechanical action to periodically refresh the outmost surface of the wafer during plating.[11] The first approach, namely, dc plating in the presence of a leveling agent has been widely practiced to obtain smooth deposits in the thick film limit, $\approx$10 to 100 micrometers, for a number of years. For the present application, idealized leveling activity should rapidly deactivate the surface before curvature inversion and bump formation occurs without substantially attenuating bottom-up feature filling. In this paper certain aspects of this approach are explored numerically. To motivate this effort a brief description of the chemical nature of the SPS-Cl-PEG system, known levelers, and plausible interactions follows.

In the SPS-Cl-PEG system the catalytic activity of the SPS accelerator has been attributed to the anionic sulfonic acid tail group that disrupts or prevents formation of the deposition rate suppressing PEG on the electrode surface while the disulfide/thiol/thiolate head group tethers or constrains the molecule to the surface.[1] Thus, a natural approach to quenching catalyst activity is to focus on disrupting the anionic tail group function and/or displacing the disulfide/thiol/thiolate head group from the surface.

Numerous leveling additives for copper deposition have been identified with most of these being associated with molecules bearing various N-functional groups including simple alkyltrimethylammonium salts,[6,13] more complex species such as crystal violet[14-16] or Janus Green B[17,18] dyes, corrosion and plating inhibitors like benzotriazole[19,20] and its derivatives,[21] and polymers such as polyethyleneimine (PEI)[22,23] or certain aromatic variants. The cationic nature of these molecules suggests an ion-pairing interaction with the anionic end group of the SPS catalyst might be a key element in leveling performance.[24] However, for many levelers, greater complexity[25] is possible as the nitrogen functional group (e.g., PEI and benzotriazole, BTA) may bear a lone pair of electrons available for interaction with electrolyte species such as protons, Cu^+, or Cu^{2+} as well as the copper electrode. Depending on the molecule, the N group can exhibit a fixed charge or, alternatively, be subject to charging by protonation. Significant differences between the transport and adsorption kinetics of small molecules vs large polyelectrolyte species would be anticipated.[26] As lithographically derived feature sizes become smaller it is also conceivable that steric and/or entropic constraints might further hinder transport of polymeric species into certain geometries. Polymeric additives are also expected to exhibit significant kinetic irreversibility during surface interactions or subsequent rearrangements.

An important aspect of leveler performance that is unrelated to feature filling per se is the extent of N incorporation in the plated solid, as such incorporation can impact relevant physical and chemical properties.[6,7] The N content can be a function of the molecular weight and functionality of the leveler and is expected to scale with the strength of the interaction of the leveler with the metal cations and/or electrode surface. For example, in one recent report the N content was found to scale with S incorporation[7] while another study indicated that incorporation ranged from negligible to significant levels depending on the nature of the leveling molecule.[6]

To develop more insight into the correlation between N functionality and leveling behavior, the effect of a simple, prototypical class of N-bearing surfactant, namely, alkyltrimethylammonium halide salt, $[(CH_3)_3RN^+A^-]$, on the metal deposition kinetics and feature filling behavior is being examined in a superfilling SPS-Cl-PEG electrolyte.[6,27] The fixed cationic charge and the absence of complexation between the leveler and Cu^+, or Cu^{2+}, simplify the evaluation of leveler-catalyst interactions. Ion-pairing between the fixed charge of the ammonium leveler head group and the sulfonic acid terminal group, coupled with hydrophobic R_{SPS}-R_{N+} alkyl chain-

* Electrochemical Society Active Member.
[z] E-mail: thomas.moffat@nist.gov

chain amphiphilic interactions, is likely to be the dominant force at play.[24] Direct chemisorption of $(CH_3)_3RN^+$ on Cu is not expected, although coadsorption in the presence of halide is anticipated.[16,28] Structured hemicylindrical or spherical-micelle physisorption of the $(CH_3)_3RN^+$ surfactants is well known,[29-32] and, upon approaching saturation, these structures should limit access of the Cu^{2+} to the electrode surface in a manner analogous to the action of adsorbed PEG. Finally, and of potential practical significance, one might anticipate minimal incorporation of $(CH_3)_3RN^+$-SPS surfactant leveler into the solid as compared to levelers with more chemically active N groups.

In this work, a series of rate equations is developed to describe the interaction between the leveler (LEV) and the accelerator (SPS) as an extension of the existing CEAC model. These equations are then used to simulate electroanalytical experiments on planar substrates and to predict feature filling in patterned wafers. Although the construct is developed in the context of copper SPS-Cl-PEG-LEV electroplating, it is believed that the underlying physics of the three additive variation of the original CEAC model is likely to be general and not necessarily limited to the specific chemical interactions and rational outlined above.

Competitive Adsorption Model

Quantitative description of the impact of catalyst-deactivating adsorbate, i.e., leveler, on the two-component CEAC model of superconformal film growth was built upon the previously published competitive adsorption model and associated kinetic parameters for the SPS-Cl-PEG system.[1] The key dynamic of the original model is the progressive displacement of adsorbed PEG from the interface by potential-dependent SPS adsorption. In the presence of a leveler two additional processes were considered: the leveler deactivates the adsorbed accelerator either by (*i*) adsorption from the electrolyte or (*ii*) lateral interactions during area reduction of surface segments that are saturated with catalyst and leveler. The invoked hierarchy of interactions stipulates that the leveler can deactivate/displace both PEG and SPS from the surface. Lacking data to the contrary, a single potential-independent rate constant, k^+_{LEV}, is used to describe the leveler-PEG and leveler-SPS displacement process. A further simplifying element is that the leveler-saturated surface was assumed to have the same metal deposition kinetics as the PEG-Cl suppressor-saturated surface; this is supported by recent experimental work in our laboratory for the case of the prototypical cationic surfactant leveler $(CH_3)_3C_{12}H_{25}N^+Cl^-$ (DTAC).[27] An important consequence is that interface motion is unaffected by the competition between leveler and PEG for surface sites; displacement or deactivation of the SPS catalyst by the leveler is the central means for altering the growth velocity and thereby the bottom-up feature filling dynamic.

The growth equation for the SPS-Cl-PEG-LEV system was taken as the sum of the surface-fraction θ_j weighted deposition rates or current density i_j for metal deposition on bare and/or fully modified surfaces; i^o_{PEG} is the exchange current density for the PEG-suppressed surface ($\theta_{PEG} = 1$); i^o_{SPS} for SPS accelerator covered surface ($\theta_{SPS} = 1$); i^o_{LEV} for leveler-covered surface ($\theta_{LEV} = 1$); and i_{FREE} for the bare surface ($\theta_{FREE} = 1$). The metal deposition rate was also taken to be proportional to the local interfacial metal ion concentration C_m. Thus the current density is written

$$i(\theta_{PEG},\theta_{SPS},\theta_{LEV},\theta_{FREE},\eta,C^o_m) = \frac{C_m}{C^o_m}\sum_j n\theta_j i^o_j\left\{\exp\left[-\frac{\alpha_j F}{RT}\eta\right] - \exp\left[\frac{(1-\alpha_j)F}{RT}\eta\right]\right\} \quad [1]$$

with j = PEG, SPS, LEV, and FREE, Faraday's constant F = 96,485 C/mol and Boltzmann's constant R = 8.314 J/mol K. Chloride is a required co-adsorbate for both the suppressor and accelerator, so these coverages should strictly be $\theta_{PEG\text{-}Cl}$ and $\theta_{SPS\text{-}Cl}$; however, since halide is plentiful in the electrolyte, the respective needs are readily met so that chloride coverage is not explicitly tracked. The deposition rate was expressed as an interface velocity normal to the surface v using Faraday's law $v = i\Omega/nF$ with Ω the molar volume of the deposited metal and n the charge of the metal ion in the electrolyte.

Electroanalytical and feature filling experiments were simulated assuming that the initial immersed surface was rapidly covered with PEG-Cl ($t = 0$, $\theta_{PEG} = 1$) and that any free sites that subsequently develop on advancing convex surfaces were rapidly, i.e., instantaneously, covered with PEG-Cl. These conditions are rationalized by the concentration of PEG relative to the other additive species combined with exposure to the PEG-enriched air-electrolyte interface during immersion prior to the onset of plating. These stipulations enable attention to be focused on the evolution of θ_{SPS} and θ_{LEV}; the limitations of such approximations will be explored elsewhere.

Mass conservation yields

$$\frac{d\theta_{SPS}}{dt} = \kappa v\theta_{SPS} + C_{SPS}k^+_{SPS}(1-\theta_{SPS}-\theta_{LEV}) - \theta_{SPS}C_{LEV}k^+_{LEV} - k^-_{SPS}(\theta_{SPS})^q \quad [2]$$

for the surface coverage of adsorbed accelerator, and

$$\frac{d\theta_{LEV}}{dt} = \kappa v\theta_{LEV} + C_{LEV}k^+_{LEV}(1-\theta_{LEV}) - k^-_{LEV}\theta_{LEV} \quad [3]$$

for the leveler coverage. The first term on the right side of the evolution Eq. 2 and 3 accounts for the impact of area change on the local coverage of the given adsorbate; this key term of the CEAC formalism is a mass conservation statement for an adsorbate that remains segregated on the surface during growth. Positive κ corresponds to a concave interface such as the bottom of a trench, while $\kappa = 0$ defines a planar surface. The second term in each equation accounts for adsorbate accumulation from the electrolyte; C_i is the concentration of the given additive adjacent to the metal/electrolyte interface and k^+_i equals the adsorption rate constant. The respective accumulation terms reflect the hierarchy of surface-binding interactions with the accelerator only able to adsorb on sites occupied by suppressor (i.e., by displacement) and the leveler adsorbing on sites occupied by either the suppressor or accelerator.

The third term in the accelerator evolution Eq. 2, which does not appear in previous CEAC models, represents deactivation of the accelerator by the adsorbing leveler; this term equals the rate at which the leveler accumulates from the electrolyte weighted by the fraction of sites where it displaces or deactivates the adsorbed SPS accelerator. Physically, the interaction could involve masking accelerator activity by forming an ion pair on the surface or displacing the accelerator into the electrolyte or into the growing solid (i.e., incorporation). The latter is consistent with recent experimental findings of enhanced accelerator incorporation in the presence of a leveler.[7] The final term in the evolution Eq. 2 and 3 quantifies the independent deactivation of the respective adsorbate species, possibly by incorporation into the growing solid or desorption of the molecule or some fragment back into the electrolyte. For the accelerator, a form consistent with the previously determined consumption of SPS during Cu deposition has been used.[1] The expression for the leveler, formally indistinguishable from Langmuir desorption, can be interpreted as a consumption or incorporation function that is first order in leveler coverage.

Importantly, the first term in Eq. 2 and 3 does not contribute to additive evolution during deposition on smooth planar electrodes; this allows conventional electroanalytical measurements on planar electrodes to be used to quantify all other terms in Eq. 1-3. In contrast, during deposition on nonplanar, e.g., lithographically patterned, surfaces, the area change terms can dominate the local response of a surface. In the case of two-component accelerator-suppressor systems, this yields the well-known bottom-up filling dynamic.[1] Significantly, in the presence of leveler, an important variation can occur. Specifically, Eq. 2 and 3 apply only as long as there is still suppressor that can be removed from the surface (i.e.,

$\theta_{SPS} + \theta_{LEV} < 1$). If the surface is fully covered with adsorbed accelerator and leveler (i.e., $\theta_{SPS} + \theta_{LEV} = 1$) and Eq. 2 and 3 yield

$$\frac{d\theta_{SPS}}{dt} + \frac{d\theta_{LEV}}{dt} > 0 \quad [4]$$

then θ_{LEV} continues to evolve according to Eq. 3, but the θ_{SPS} must now accommodate the evolution of the leveler according to

$$\frac{d\theta_{SPS}}{dt} = -\frac{d\theta_{LEV}}{dt} \quad [5]$$

It is through Eq. 5 that adsorbed accelerator is deactivated by adsorbed leveler during area reduction in suppressor-free regions. Note this inverse of the curvature enhanced accelerator coverage process is entirely distinct from the classical picture of leveling known as diffusion-adsorption-consumption models.[33-39] From this perspective, the CEAC acronym can be generalized to stand for any curvature enhanced adsorbate coverage process. As with early CEAC models, area change effects can dominate over coverage differentiation arising from boundary layer transport controlled process. This naturally follows from the relevant length scales involved, i.e., coverage changes due to rapid area change within submicrometer ($\sim$100 nm) features overwhelm any lateral variations associated with diffusional fluxes over the hydrodynamic boundary layer (10–100 μm). In the modeling that follows, at locations where the leveler coverage saturates ($\theta_L = 1$) and Eq. 3 yields $d\theta_{LEV}/dt > 0$, $\theta_L = 1$ was imposed and any excess leveler was modeled as incorporated into the growing solid; it could alternatively have been modeled as desorbed into the electrolyte with appropriate modification of mass conservation boundary conditions at the interface.

Electroanalytical Simulations

Conventional electroanalytical methods are widely used to characterize plating electrolytes for both process development and control. Previous investigations have shown that characteristics such as hysteretic voltammetric (potential-current: η-*i*) and rising chronoamperometric (current-time: *i*-*t*) traces are important indicators of superfilling performance in a variety of chemically distinct systems, e.g., copper,[1] silver,[40] and gold.[41] Indeed, the CEAC construct provides a causal quantitative bridge between the two. Thus, the impact of leveler addition on the voltammetric and chronoamperometric response of the SPS-Cl-PEG-LEV system is examined. The SPS concentration was fixed at 50 μmol/L since this is known to permit effective superfilling of submicrometer features. A brief survey of the literature indicates that levelers are utilized over a broad concentration range between 0.5 and 500 μmol/L.[4-18] Simulations were performed as a function of leveler concentration C_{LEV} while all other parameters were fixed. Depletion effects for all species were evaluated using the steady-state hydrodyamic boundary layer approximation. The interface concentrations of SPS and the LEV species were thus defined by mass balance

$$C_{SPS} = \frac{C_{SPS}^{bulk}}{1 + \frac{k_{SPS}^{+}\Gamma_o^{SPS}\delta(1 - \theta_{SPS} - \theta_{LEV})}{D_{SPS}}}$$

$$\text{and } C_{LEV} = \frac{C_{LEV}^{bulk}}{1 + \frac{k_{LEV}^{+}\Gamma_o^{LEV}\delta(1 - \theta_{LEV})}{D_{LEV}}} \quad [6]$$

where the Cu^{2+} depletion gradients establish the boundary layer thickness, δ, within 30 s of the onset of deposition. Values for the diffusion coefficient, D_{LEV}, and the saturation surface coverage Γ_{LEV} for a variety of $(CH_3)_3RN^+$ molecules have been reported.[42] The values are close to those previously used for SPS and thus for simplicity the same numbers are used. Several detailed thermochemical and structural studies of $(CH_3)_3RN^+$ adsorption are available. For example, on negatively charged silica surfaces the adsorption dynamics are tightly correlated with the critical micelle concentration (CMC), electrolyte identity, and concentration.[42-44] The structure of such layers is also sensitive to the surface charge.[30-32] In the case of decyltrimethylammonium chloride (DTAC) in water the CMC is 20 mM although salting-out can shift the CMC by at least an order of magnitude.[42,45] In the present case, preliminary η-*i* experiments in the SPS-Cl-PEG-DTAC system were used to constrain the choice of the adsorption and deactivation kinetics.[27] If the leveler deactivation process is interpreted as a simple desorption step then the ratio k_{LEV}^{+}/k_{LEV}^{-} corresponds to the Langmuir adsorption constant, *K*, the reciprocal of which was found to be ≈28 μmol/L. Table I lists all relevant kinetic parameters.

Table I. Parameters used for the calculations.

Parameter	Value
α_{PEG} (and α_{LEV})	0.5
α_{SPS}	0.4
i_{PEG}^{o} (and i_{LEV}^{o})	0.03 mA cm^{-2}
i_{SPS}^{0}	2.25 mA cm^{-2}
T	298 K
η (fixed for feature filling)	−0.25 V
C_m^o	2.4×10^{-4} mol/cm^3
C_{SPS}^{bulk}	50×10^{-9} mol/cm^3
C_{LEV}^{bulk}	Variable
D_m	4×10^{-6} cm^2 s^{-1}
D_{SPS} (and D_{LEV})	4×10^{-6} cm^2 s^{-1}
δ	9.87×10^{-3} cm
Ω	7.1 cm^3 mol^{-1}
n	2
Γ_o^{SPS} (and Γ_o^{LEV})	6.35×10^{-10} mol cm^{-2}
k_{SPS}^{+}	$f(\eta)$ see Ref. 1
k_{SPS}^{-}	$f(\eta)$ see Ref. 1
q	1.65
k_{LEV}^{+}	1.8×10^4 cm^3 mol^{-1} s^{-1}
k_{LEV}^{-}	5×10^{-4} s^{-1}
Trench depth	4×10^{-5} cm
Width at half trench depth	2.7×10^{-5} cm
ϕ (sidewall tilt)	5°

The effect of the leveler on the voltammetric and chronoamperometric behavior of the SPS-Cl-PEG-LEV system is summarized in Fig. 1 and 2. The hysteretic voltammetric curve in the leveler-free electrolyte reflects the progressive displacement of the rate suppressing PEG by potential-dependent SPS adsorption.[1] Addition of the DTAC leveler leads to a decrease in the hysteretic response as well as a shift toward more negative potentials reflecting the quenching of the SPS activity. The intersection of the forward and reverse sweep for the more concentrated leveler electrolytes, e.g., 100–400 μmol/L, is an unambiguous indication that leveler adsorption is under some kinetic constraint, i.e., the crossing point would not exist for fully equilibrated Langmuir adsorption of the leveler. The kinetic restraint on competitive leveler adsorption is also revealed by the maxima in the corresponding chronoamperometry simulations shown in Fig. 2a.

Deposition at an overpotential of −0.25 V was examined since this corresponds to an effective value for superfilling in the SPS-Cl-PEG system. Significantly, for leveler concentrations below $\sim$50 μmol/L, there is negligible impact on the metal deposition rate during the ≈100 s time scale that corresponds to submicrometer feature filling experiments.[1] This is because i_{LEV}^{o} and i_{PEG}^{o} are approximately equal and much less than i_{SPS}^{o} so that leveler accumulation does not affect the current density until its adsorption begins to impact θ_{SPS} evolution. The time scales for accelerator and leveler accumulation are most obvious through the maximums in the chronoamperometric transients in Fig. 2 whereby the rapid rise due to accelerator accumulation is replaced by subsequent decay through leveler accumulation and the leveler-accelerator deactivation term,

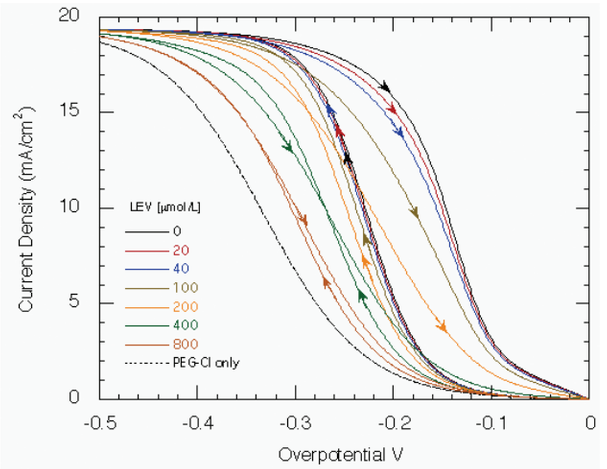

Figure 1. Slow scan voltammetry reveals the influence of leveler additions on copper deposition rate in an electrolyte comprised of 1.8 mol/L H_2SO_4 + 0.25 mol/L $CuSO_4$ + 88 μmol/L PEG + 1 mmol/L NaCl + 50 μmol/L SPS + x μmol/L LEV. For reference, a η-i trace for copper deposition in a PEG-Cl (i.e., SPS- and LEV-free) electrolyte is shown. Scan rate is 1 mV/s.

$\theta_{SPS}k^+_{LEV}C^i_{LEV}$, in Eq. 2. Transients predicted using Eq. 1-3 with kinetics from Table I are shown with associated coverages θ_{SPS} and θ_{LEV} in Fig. 3a and b for leveler concentrations of 40 and 400 μmol/L, respectively.

Shape-Change Simulations

The competitive adsorption model and associated kinetics were also used to examine the effect of leveler concentration on shape evolution during deposition in a Damascene trench geometry. Two different deposition conditions were examined. The first case follows the evolution of an electrode derivatized with fixed initial SPS coverage of $\theta_{SPS} = 0.025$ followed by deposition in the presence of PEG-Cl-LEV. This choice permitted isolation of leveler interactions with an adsorbed accelerator free of the kinetics of accelerator adsorption. Such superfilling with a preadsorbed accelerator has been previously demonstrated to also be fully quantifiable by the CEAC

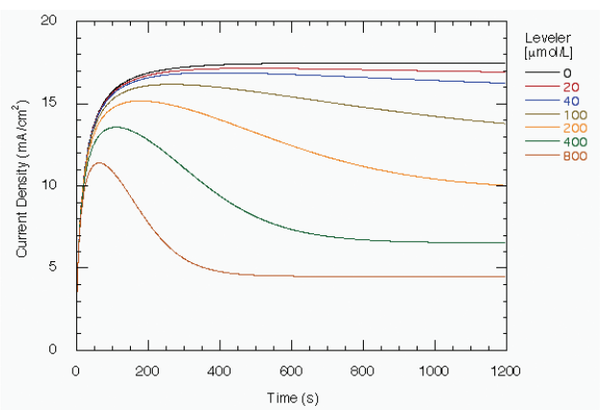

Figure 2. The influence of leveler concentration during potentiostatic (−0.25 V) copper deposition in 1.8 mol/L H_2SO_4 + 0.25 mol/L $CuSO_4$ + 88 μmol/L PEG + 1 mmol/L NaCl + 50 μmol/L SPS + x μmol/L LEV. Note, for leveler concentrations less than ~40 μmol/L a relatively small perturbation on the metal deposition kinetics is apparent during the first 100 s that includes typical feature filling times.

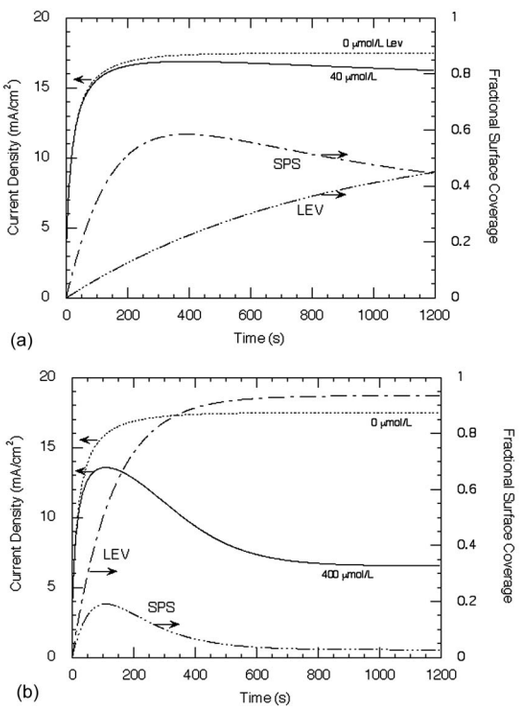

Figure 3. Simulated current-time transients and corresponding time evolution of θ_{SPS} and θ_{LEV} for the chronoamperometric traces shown in Fig 2; (a) 20 μmol/L LEV, (b) 400 μmol/L LEV.

mechanism.[1] In the second set of simulations, the initial values of θ_{SPS} and θ_{LEV} were both set to zero and allowed to evolve during Cu deposition in a SPS-Cl-PEG-LEV electrolyte.

Simulations were performed using a level set formulation of the CEAC model[46] within a Python framework developed at NIST that is known as FiPy.[47] In contrast to the electroanalytical simulations, the full time-dependent diffusion equations for transport of Cu^{2+}, SPS, and LEV within the boundary layer and unfilled region of the trench were evaluated using

$$\frac{\partial C_j}{\partial t} = D_j \nabla^2 C_j \qquad [7]$$

with uniform bulk concentrations at the start of deposition ($t = 0$). The remaining boundary conditions were obtained by imposing mass conservation along the growth surface. For the metal this yields

$$D_M \nabla C_M \cdot \hat{n} = v\left(\frac{1}{\Omega}\right) \qquad [8]$$

which equates the metal deposited on the surface with that arriving from the electrolyte.

Conservation of the additives at the growth surface is enforced by equating that arriving from the electrolyte with that adsorbing on the surface according to

$$D_{SPS} \nabla C_{SPS} \cdot \hat{n} = \Gamma C_{SPS} k^+_{SPS}(1 - \theta_{SPS} - \theta_{LEV})$$

$$D_{LEV} \nabla\ C_{LEV} \cdot \hat{n} = \Gamma C_{LEV} k^+_{LEV}(1 - \theta_{LEV}) \qquad [9]$$

where $\hat{n}$ is the local unit normal of the surface (pointing into the electrolyte). Implicit in Eq. 9 is the assumption that adsorbates eliminated through consumption or during area reduction of saturated surfaces are buried (or deactivated) so that they do not appear in the mass balance. In the case of slow interface kinetics and negligible leveler depletion effects, Langmuir desorption represents a

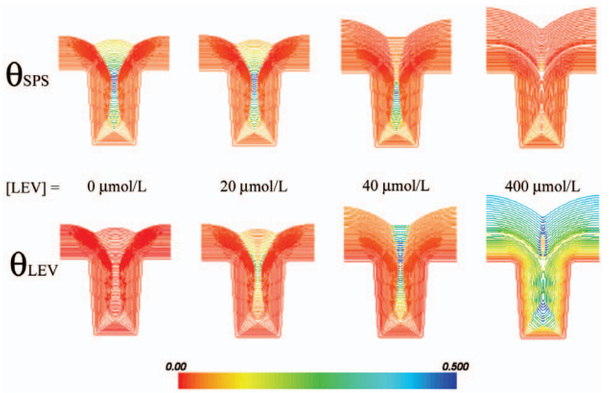

Figure 4. Feature filling contours for copper deposition on SPS-derivatized electrodes where $\theta_{SPS}^{t=0} = 0.025$. The contours are colorized to reflect the local θ_{SPS} (top row) and θ_{LEV} (bottom row), respectively. Potentiostatic copper deposition in a PEG-Cl-LEV electrolyte was simulated as a function of leveler concentration, 0, 20, 40, and 400 μmol/L as marked.

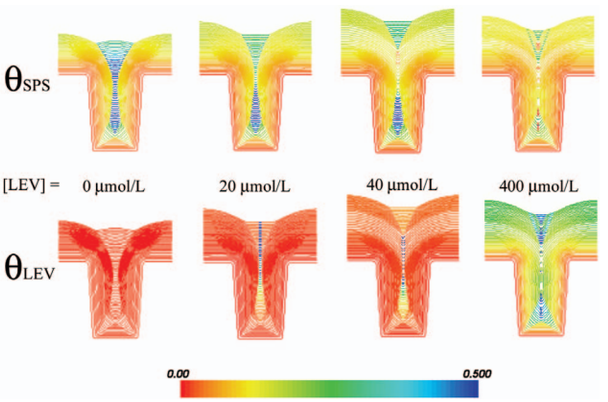

Figure 5. Feature filling contours for copper deposition on a PEG-Cl saturated surface (i.e., $\theta_{SPS}^{t=0} = 0$). The contours are colorized indicating θ_{SPS} (top row) and θ_{LEV} (bottom row) evolution as a result of accumulation from the electrolyte and area change. Potentiostatic copper deposition in a PEG-Cl-SPS-LEV electrolyte was simulated as a function of leveler concentration, 0, 20, 40, and 400 μmol/L as marked.

viable alternative interpretation. Experiments will be required to distinguish between the two paths.

Simulations of superfilling in the PEG-Cl-LEV electrolyte using an SPS-derivatized substrate are shown in Fig. 4. The initial SPS coverage was 0.025, and the growth contours are colorized to reflect local coverages of SPS (top) and LEV (bottom). The enrichment of accelerator on concave sections and resulting void-free bottom-up filling and overfill bump are evident. Upon the addition of 20, 40, and 400 μmol/L leveler to the PEG-Cl plating electrolyte, SPS deactivation and its consequences on feature filling are progressively more apparent. For 20 μmol/L leveler, enrichment of the adsorbed leveler due to area reduction is evident where the bottom surface approaches the top of the feature in the colorized leveler contour plot, however, the impact on the filling behavior is not significant. Doubling the leveler concentration to 40 μmol/L results in more significant buildup of the leveler coverage and significant attenuation of the SPS coverage during filling toward the top of the feature. While the bottom-up filling dynamic is still evident, the leveler accumulation, mostly due to area change, is such that bump formation does not occur. The final concave surface profile indicates that the leveler concentration in the electrolyte is slightly in excess of the optimum value required for obtaining a planar surface. Examination of the leveler coverage shows that, while $\theta_{LEV} < 0.1$ on the free surface, $\theta_{LEV} \approx 0.5$ at the center of the feature. This unambiguously demonstrates the overwhelming importance of leveler enrichment by the CEAC area change mechanism. Increasing the leveler concentration an order of magnitude to 400 μmol/L results in extensive leveler adsorption that completely eliminates the bottom-up SPS-derived filling dynamic. This results in subconformal growth and void or seam formation in the final structure.

Feature filling contours for the case of deposition in the SPS-Cl-PEG-LEV system for concurrent SPS and LEV adsorption are shown in Fig. 5. Shape evolution with SPS adsorbing during metal deposition is similar to that observed with the preadsorbed SPS in Fig. 4; bottom-up filling is evident as is subsequent bump formation. The chief distinction from the previous simulations is the higher coverage of accelerator on the free-surface due to the continuous SPS accumulation from the electrolyte during metal deposition. The net effect is more rapid filling and a narrowing of the space between the sidewalls during the latter stages of bottom-up filling. This is tantamount to a slight reduction of the upper bound of feature aspect ratio that can be filled as compared to the derivatized case.

In the presence of 20 μmol/L leveler the bottom-up filling dynamic and subsequent bump formation are significantly attenuated. The substantial influence of area change on leveler coverage within the trench as compared to the small contribution derived from electrolyte adsorption (e.g., on the neighboring planar field) is evident in the colorized θ_{LEV} contours. This is consistent with the absence of a significant impact of leveler accumulation on the deposition rate during chronoamperometry (i.e., Fig. 3a) during the ≈100 s time scale of feature filling. Doubling the leveler concentration to 40 μmol/L results in failure of bottom-up feature filling for the present conditions. Two small voids are indicated by the discontinuities in the colorized leveler contours along the centerline. A further increase in the leveler concentration to 400 μmol/L leads to accentuated voiding. This occurs because the area-change induced increase of leveler coverage on the concave bottom of the trench preferentially deactivates SPS on this surface while significant SPS continues to accumulate on the side walls. The resulting pinch-off is revealed by the discontinuities in the colorized contours along the centerline.

Interface motion during superfilling is largely dominated by catalyst coverage and the impact of leveler on this coverage. The leveler deactivates the adsorbed accelerator either by adsorption from the electrolyte or by lateral interactions during area reduction. From the perspective of controlling bump formation in submicrometer features, area change plays the dominant role with the caveat that suitable leveler coverage is attained prior to significant feature filling. Alternatively stated, the details of the initial leveler adsorption processes (k_{LEV}+, D_{LEV}, C_{LEV}) are of secondary importance as long as enough leveler accumulates on the surface profile before significant area reduction occurs. This finding helps explain an unusual aspect in filling images reported for an industrial three-component copper process.[7] Specifically, in the absence of leveler a huge buildup occurs over high density regions of high aspect ratio (~3) features whereas little overburden is evident over neighboring low aspect features, as shown in Fig. 6; in contrast, in the presence of a high concentration of leveler the situation is reversed, with greater buildup over low aspect ratio features. Whereas the former observation was explained through the impact of area change on the accelerator coverage within the original CEAC mechanism, the latter observation can now be explained by the CEAC area reduction effect on leveler coverage. In particular, due to the initially large surface area and subsequent area reduction, a higher enrichment of leveler, and correspondingly low coverage of accelerator, is obtained on the surface over regions of more densely packed fine features after filling. It is unclear how traditional diffusion-adsorption-consumption models of leveling could explain the inversion in overburden with leveler concentration. Detailed simulations of three-component (suppressor-accelerator-leveler) interactions on feature filling as a function of pattern density remain to be developed. How-

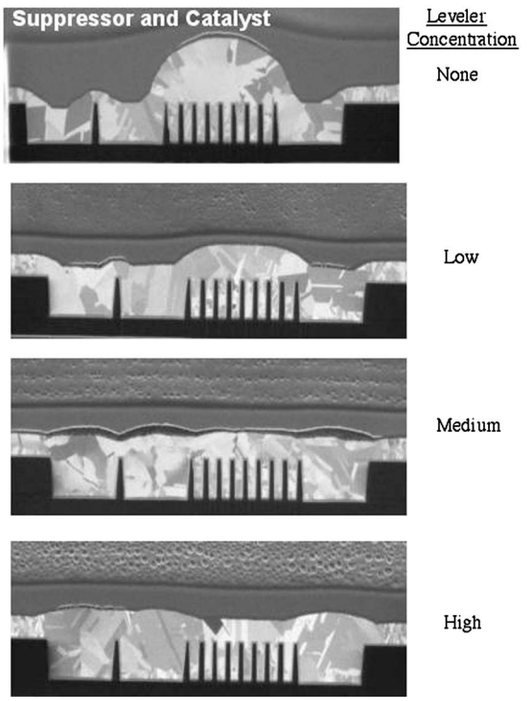

Figure 6. Attenuation of bump formation during copper deposition by the addition of a leveler to an electrolyte containing a suppressor, brightener, and progressively higher leveler concentrations. Note the inversion of the overburden at the highest leveler concentration. As noted in text, this can be explained within the extended CEAC model developed herein by leveler enrichment due to area change. (Image provided by C. Witt courtesy of Enthone, Inc.)

ever, it is clear that the area change term associated with the curvature enhanced adsorbate coverage model will be important to any description of leveling in the filling of submicrometer features.

Conclusions

The curvature enhanced adsorbate coverage or CEAC mechanism has been further generalized to describe the morphological evolution during electrodeposition the from three-component suppressor-accelerator-leveler chemistry. The formalism provides a quantitative means of exploring the impact of leveling additives on overfill bump height in copper Damascene superfill. The CEAC leveling mechanism is completely distinct from the well-known diffusion-adsorption-consumption model of leveling. The combination of electroanalytical and shape-change simulations demonstrates the importance of area change effects in understanding the action of surfactant levelers. The simulation tools may also be used in combination with experiments to identify and optimize electrolytes for a given application.

National Institute of Standards and Technology assisted in meeting the publication costs of this article.

References

1. T. P. Moffat, D. Wheeler, M. Edelstein, and D. Josell, *IBM J. Res. Dev.*, **49**, 19 (2005).
2. Q.-T. Jiang, A. Frank, B. Carpenter, R. Carpio, T. Ritzdorf, R. A. Auger, K. Pfeifer, and J. D. Luttmer, in *Proceedings of Advanced Metallization Conference 2000*, A. J. McKerrow, Y. Shacham-Diamand, S. Zaima, and T. Ohba, Editors, MRS, Warrendale, PA (2001); A. Frank, Q. T. Jiang, L. Chen, B. Carpenter, R. Carpio, T. Ritzdorf, and K. Pfeifer, in *Proceedings of Advanced Metallization Conference*, 2000, D. Edelstein, G. Dixit, Y. Yasuda, and T. Ohba, Editors, p. 181, MRS, Warrendale, PA (2000).
3. Y. H. Im, M. O. Bloomfield, S. Sen, and T. S. Cale, *Electrochem. Solid-State Lett.*, **6**, C42 (2003).
4. B. Zheng, R. He, B. Mikkola, J. Wang, C. Long, C. Yu, Z.-W. Sun, E. Step, J. Chen, R. Emamai, Z. A. Wang, R. Nayak, T. Taylor, and G. Dixit, in *Proceedings of Advanced Metallization Conference 2001*, A. J. McKerrow, Y. Shacham-Diamand, S. Zaima, and T. Ohba, Editors, p. 197, *MRS*, Warrendale, PA (2001).
5. T. Haba, T. Itabashi, H. Akahoshi, and H. Miyazaki, pg 361, in *Advanced Metallization Conference 2002*, B. M. Melnick, T. S. Cale, S. Zaima, and T. Ohta, Editors. p. 361, MRS, Warrendale, PA (2003).
6. J. Reid, E. Webb, J. Sukamto, Y. Takada, and T. Archer, in *Electrochemical Processing in ULSI and MEMS*, H. Deligianni, S. T. Mayer, T. P. Moffat, and G. R. Stafford, Editors, PV 2004-17, p. 184, The Electrochemical Society Proceedings Series, Pennington, NJ (2005).
7. C. Witt, J. Srinivasan, and R. Carpio, in *Electrochemical Processing in ULSI and MEMS*, H. Deligianni, S. T. Mayer, T. P. Moffat, and G. R. Stafford, Editors, PV 2004-17, p. 57, The Electrochemical Society Proccedings Series, Pennington, NJ (2005).
8. M. Hasegawa, Y. Negishi, T. Nakanishi, and T. Osaka, *J. Electrochem. Soc.*, **152**, C221 (2005).
9. S.-K. Kim, S. Hwang, S. K. Cho, and J. J. Kim, *Electrochem. Solid-State Lett.*, **9**, C25 (2006).
10. S. K. Cho and J. J. Kim, *Abstract 580, The Electrochemical Society, Meeting Abstracts*, Vol. 2005-2, Los Angeles, CA, Oct 16-21, (2005).
11. B. M. Basol, *J. Electrochem. Soc.*, **151**, C765 (2004).
12. M. X. Yang, D. X. Mao, C. M. Yu, J. Dukovic, and M. Xi, *Solid State Technol.*, **46**, 37 (2003).
13. E. D. Eliadis and R. C. Alkire, *J. Electrochem. Soc.*, **145**, 1218 (1998).
14. W. Plieth, *Electrochim. Acta*, **37**, 2115 (1992).
15. N. Batina, D. M. Kolb, and R. J. Nichols, *Langmuir*, **8**, 2572 (1992).
16. M. Kunitake, N. Batina, and K. Itaya, *Langmuir*, **11**, 2337 (1995).
17. Y. Cao, P. Taephaisitphongse, R. Chalupa, and A. West, *J. Electrochem. Soc.*, **148**, C466 (2001); P. Taephaisitphongse, Y. Cao, and A. C. West, *J. Electrochem. Soc.*, **148**, C492 (2001).
18. W.-P. Dow, H.-S. Huang, M.-Y. Yen, and H.-C. Huang, *J. Electrochem. Soc.*, **152**, C425 (2005).
19. J. K. Prall and L. L. Shreir, *Trans. Inst. Met. Finish.*, **41**, 29 (1964).
20. M. E. Biggin and A. A. Gewirth, *J. Electrochem. Soc.*, **148**, C339 (2001).
21. T. Y. B. Leung, M. C. Kang, B. F. Corry, and A. A. Gewirth, *J. Electrochem. Soc.*, **147**, 3326 (2000).
22. M. Wuensche, W. Dahms, H. Mayer, and R. Schumacher, *Electrochim. Acta*, **39**, 1133 (1994).
23. S.-K. Kim, D. Josell, and T. P. Moffat, In preparation.
24. A. Tulpar and W. A. Ducker, *J. Phys. Chem. B*, **108**, 1667 (2004).
25. C. F. J. Faul and M. Antonietti, *Adv. Mater.*, **15**, 673 (2003).
26. R. R. Netz and D. Andelman, in *Encyclopedia of Electrochemistry-V1, Thermodynamics and Electrified Interfaces*, E. Gileadi, M. Urbakh, M. Stratmann, and A. J. Bard, Editors, p. 282, Wiley-VCH, Weinheim (2002).
27. S.-K. Kim, D. Wheeler, D. Josell, and T. P. Moffat, In preparation.
28. C. Safarowsky, A. Rang, C. A. Schalley, K. Wandelt, and P. Broekmann, *Electrochim. Acta*, **50**, 4257 (2005).
29. H. N. Patrick, G. G. Warr, S. Manne, and I. Aksay, *Langmuir*, **15**, 1685 (1999).
30. I. Burgess, C. A. Jeffrey, X. Cai, G. Szymanski, Z. Galus, and J. Lipkowski, *Langmuir*, **15**, 2607 (1999).
31. I. Burgess, V. Zamlynny, G. Szymanski, J. Lipkowski, J. Majewski, G. Smith, S. Sitija, and R. Ivkov, *Langmuir*, **17**, 3355 (2001).
32. M. Petri and D. M. Kolb, *Phys. Chem. Chem. Phys.*, **4**, 1211 (2002).
33. C. Madore, M. Matlosz, and D. Landolt, *J. Electrochem. Soc.*, **143**, 3927 (1996).
34. C. Madore and D. Landolt, *J. Electrochem. Soc.*, **143**, 3936 (1996).
35. A. C. West, *J. Electrochem. Soc.*, **147**, 227 (2000).
36. R. Chalupa, Y. Cao, and A. C. West, *J. Appl. Electrochem.*, **32**, 135 (2002).
37. J. Dukovic, in *Advances in Electrochemical Science and Engineering*, H. Gerischer and C. W. Tobias, Editors, p. 117, VCH Publications, Weinham (1994).
38. S. I. Krichmar, *Elektrokhimiya*, **1**, 858 (1965).
39. D. Roha and U. Landau, *J. Electrochem. Soc.*, **137**, 824 (1990).
40. B. C. Baker, M. Freeman, B. Melnick, D. Wheeler, D. Josell, and T. P. Moffat, *J. Electrochem. Soc.*, **150**, C61 (2003).
41. D. Josell, D. Wheeler, and T. P. Moffat, *J. Electrochem. Soc.*, **153**, C11 (2006).
42. R. Atkins, V. S. J. Craig, E. J. Wanless, and S. Biggs, *J. Colloid Interface Sci.*, **266**, 236 (2003).
43. S. B. Velegol, B. D. Fleming, S. Biggs, E. J. Wanless, and R. D. Tilton, *Langmuir*, **16**, 2548 (2000).
44. R. Atkins, V. S. J. Craig, and S. Biggs, *Langmuir*, **16**, 9374 (2000).
45. B. L. Bales and R. Zana, *J. Phys. Chem. B*, **106**, 1926 (2002).
46. D. Wheeler, D. Josell, and T. P. Moffat, *J. Electrochem. Soc.*, **150**, C302 (2003).
47. D. Wheeler, J. Guyer, and J. A. Warren, *FiPy: A Finite Volume PDE Solver Using Python*. http://www.ctcms.ist.gov/fipy/